

## **Distinguishing and identifying point and extended defects in DLTS measurements**

Ł. GELCZUK\*, M. DĄBROWSKA-SZATA, G. JÓŹWIAK

Faculty of Microsystem Electronics and Photonics, Chair of Advanced Electronic Engineering,  
Wrocław University of Technology, Janiszewskiego 11/17 St., 50-372 Wrocław, Poland

Convenient and simple criteria are proposed enabling one to distinguish between deep level point and extended defects (e.g. dislocations) in DLTS measurements. The approach is based on earlier reports of several authors and on our own experiences in the field of DLTS data analysis for III–V semiconductors. It consists of standard DLTS measurements widened by line shape and line behaviour analysis, as well as capture kinetics measurements. In the first part, the paper presents a survey of the literature on the analysis of DLTS signals originating from dislocations. In the second part, selected experimental data on distinguishing and identifying deep point and extended defects, in GaAs/GaAs and InGaAs/GaAs heterostructures, are presented.

Key words: *defect identification; deep levels; point defects; extended defects; DLTS*

### **1. Introduction**

One of the reasons why semiconductors find so wide applications in the production of electrical and optical devices is the possibility of modifying their electronic properties by incorporating small fractions of impurities or other defects. Lattice defects are needed for doping the material with shallow, hydrogenic donors and acceptors in order to determine the majority carrier type and concentration. The carrier mobility can usually be controlled as well. For this reason, the ability of controlling defects is immensely important. Therefore, at first it is necessary to master the technological processing of bulk materials with the least number of defects, and then the process of introducing a required number of defects during the growth or after the growth of the semiconductor crystal.

In addition to these so-called desired defects, there are a wide range of undesired defects. In contrast to the hydrogenic, delocalised electron states of dopants, unde-

---

\*Corresponding author, e-mail: lukasz.gelczuk@pwr.wroc.pl

sired lattice defects are characterized by highly localized states, usually situated deep in the band gap, but also, as we know today, even close to the valence or conduction band edges. They are commonly called “deep level defects”. Examples of such deep level point defects are some impurities, vacancies, interstitials, or their clusters. Deep level defects have larger capture cross sections than hydrogenic shallow defects and in most cases determine the minority carrier lifetime. Therefore, these defects play an important role in manufacturing high-speed electronic and optoelectronic devices. Defect investigation and characterization are interesting from the cognitive and practical point of view, because they decide about the effective production of perfect semiconductor devices.

In contrast to deep point defects, spatially extended, many-electron defects form deep lying, closely spaced electronic states in the band gap. Examples of such defects are dislocations, grain boundaries, precipitates, and surface and interface states. Extended defects are known to significantly affect charge-carrier mobility and lifetime. Moreover, they can interact with point defects. By acting as sinks and sources for intrinsic point defects and segregation centres for impurities, they can create detrimental effects in microelectronic devices. The ability of extended defects to sink impurities, however, is utilized in removing impurities from the crystal, a technique known as “gettering of impurities”.

Recently Weber [1] suggested that the proper understanding of defects in semiconductors usually requires the following steps: (i) defect observation and characterization, (ii) defect identification, (iii) defect control, (iv) estimation of the influence of defects on device performance.

The first two steps determine the application area of electrical and optical spectroscopy, such as deep level transient spectroscopy (DLTS), electron beam induced current (EBIC), impedance spectroscopy (IS), and photoluminescence (PL). Structural analysis by X-ray diffraction (XRD), transmission electron microscopy (TEM), and scanning electron microscopy (SEM) are frequently employed as well. These methods are particularly essential in the case of extended defects [1]. The thorough understanding of the nature of a particular defect and its identification usually involve a combination of various methods.

Deep level transient spectroscopy is currently one of the most widely used methods for studying deep level defects in semiconductors [2]. Although the DLTS technique has been primarily developed and well-established for characterizing simple point defects (impurities, vacancies) in semiconductor materials, it can also be applied for studying extended defects such as dislocations, grain boundaries, or precipitates [3].

Over the last two decades, attempts at analysing the DLTS signal coming from dislocations in different semiconductor materials have been made by many authors [3–13]. Today our knowledge on this subject is sufficiently rich for properly examining the odd features of electron emission from dislocations and for distinguishing them from isolated point defects in DLTS measurements. Nevertheless, this requires a careful and accurate analysis, because other phenomena can affect the DLTS signal. In this paper, we discuss possibilities of applying DLTS measurements to characterize

electronic states at dislocations and we propose a simple way to distinguish deep level extended defects (e.g. dislocations) from point defects.

## 2. Deep level transient spectroscopy – theory

Deep level transient spectroscopy, developed by Lang and co-workers in 1974 [2], is considered to be a powerful and versatile capacitance technique for characterizing deep level defects in semiconductors. It provides all the important defect parameters, such as the thermal activation energy ( $E_a$ ), electron- and hole-capture cross sections ( $\sigma_{n,p}$ ), and defect concentration ( $N_T$ ). The DLTS technique relies on temporal capacitance transients (typically exponential in the case of point defects), which occur after a rapid bias change of a Schottky diode or  $p^+n-n^+p$ -junction. A reverse bias changes the width of the space-charge region in the diode or junction, and when deep levels are present, they are detected by their contribution to charge redistribution in the depletion region, resulting in a change of capacitance, i.e. capacitance transients [2, 14].

The dynamic process of electron capture and emission by deep traps can be described in terms of a capture cross section  $\sigma_n$  and emission rate  $e_n$ . On the basis of the principle of detailed balance, it can be shown that the emission rate is related to the capture cross section by the following equation [2, 14]:

$$e_n = \sigma_n v_{th} N_c \exp\left(-\frac{E_C - E_T}{kT}\right) \quad (1)$$

where  $v_{th}$  is the thermal velocity of electrons,  $N_c$  is the effective density of states in the conduction band, and  $E_C - E_T$  determines the energy level position in the band gap in relation to the conduction band edge (i.e. activation energy). A similar relation can be derived in the case of the emission and capture of holes. The inverse of the emission rate is called the emission time constant ( $\tau_e$ ) of the capacitance transient and it is generally known to satisfy the following relation [15]:

$$C(t) = C_0 \left[ 1 - \frac{n_T(0)}{2N_D} \exp\left(-\frac{t}{\tau_e}\right) \right] \quad (2)$$

where  $C_0$  is the capacitance of the original reverse bias,  $n_T(0)$  is the original number of electrons per unit volume occupying the trap level during the transient,  $N_D$  is the doping concentration, and  $t$  is the time. It follows that if the doping concentration is known,  $n_T(0)$  can be obtained, and that for a sufficiently long filling pulse time it describes the trap concentration  $N_T$ .

By analysing emission kinetics as a function of temperature, the activation energy of deep traps can be obtained from DLTS measurements. In practice, different constant rate windows (or lock-in frequencies) are used, which change the DLTS peak positions on the temperature scale and allows  $e_n$  to be evaluated. Temperature scans

taken for several rate windows (lock-in frequencies) make it possible to construct Arrhenius plots, i.e. plots of the emission rates divided by the temperature squared ( $e_n/T^2$ ) versus the reciprocal of temperature ( $1/T$ ), for each of the peaks. Finally, the values of activation energy and capture cross section (frequently called “apparent”) can be easily evaluated from the slope of the Arrhenius plot and its intersection with the emission rate axis, respectively.

The DLTS technique allows us to study the electric field dependence of the emission rate, thermally activated capture cross section, and concentration distribution profiles of the deep traps as well.

The activation energy is composed of a change in enthalpy and entropy [7, 14]. The entropy term, however, is frequently neglected and the ionisation enthalpy is assumed to be a good approximation to the ionisation energy. The ionisation energy of traps can be lowered in strong electric fields, for example by the Poole–Frenkel effect [14]. Therefore, the electric field dependence of the emission rate has to be taken into account, because neglecting this effect may lead to serious misinterpretations in the determination of deep level parameters. On the other hand, it can yield a lot of useful information on the nature of deep traps. In DLTS measurements, the influence of the electric field on the emission rate manifests itself by a shift of the DLTS peak maximum towards lower temperatures on increasing the value of the electric field. The value of the electric field is established by selecting two filling pulse heights ( $U_1$ ,  $U_2$ ) in so-called double correlation DLTS (DDLTS) [16].

When the capture process is temperature dependent for deep levels, the capture cross section can be expressed in terms of a capture barrier [14, 17]:

$$\sigma_n = \sigma_{n\infty} \exp\left(-\frac{E_B}{kT}\right) \quad (3)$$

where  $\sigma_{n\infty}$  is the capture cross section at infinite temperature ( $T \rightarrow \infty$ ) and  $E_B$  is the height of the capture barrier, which has to be overcome by free carriers in order to be captured by a trap. A thermally activated capture cross section can be investigated by measuring the DLTS peak amplitude for different widths of filling time pulses  $t_p$  at a constant temperature. The capture cross sections at different temperatures can be extracted from a specific fitting procedure [18].

The depth distribution of deep level concentration can also be measured by DDLTS, using two filling pulses with the same widths and different amplitudes, at a given rate window and constant temperature corresponding to the maximum of the DLTS peak of a selected level. The spatial resolution of the depth profile measurements is set by the constant value of  $\Delta U = U_1 - U_2$ , and their range by the value of the reverse bias  $U_R$ .

In spite of the DLTS possibilities mentioned above, this method requires some caution when analysing results. Occasionally, some phenomena can disturb or even forcibly change the DLTS signal coming from deep traps. This reservation is especially connected with the study of extended defects (e.g. dislocations) by means of the

DLTS technique. In the next sections, we discuss some peculiar features of the DLTS signal coming from dislocations, such as a change in the DLTS line shape, DLTS line behaviour, as well as non-exponential capacitance transients. The impact of other frequently observed features of contemporary semiconductor crystals, generally known as distorting factors of the classical DLTS behaviour, will also be discussed.

### 3. DLTS line amplitude shape analysis

A frequently observed feature of DLTS lines is a difference in the shape of peaks corresponding to particular deep level defects. This difference arises from the fact that in the case of isolated point defects one can usually observe narrow and symmetric peaks, while the DLTS line peaks associated with extended defects always show symmetric or asymmetric broadening. For these reasons, DLTS data for extended defects cannot be interpreted unambiguously.

The features mentioned above are due to the fact that in a conventional DLTS analysis simple point defects are known to provide exponential capacitance transients, corresponding to electron emission from traps. On the other hand, specific non-exponential capacitance transients are often observed for some deep levels. The origin of non-exponential transients is mainly attributed to the formation of dislocations or dislocation-related defects in semiconductor materials as a result of the repulsive Coulombic barriers associated with such defects (see Sec. 5).

Kimerling and Patel [4] were the first to find asymmetrically broadened DLTS lines, which were associated with dislocations in plastically deformed (PD) n-type and p-type Si that survived annealing at high temperatures. Very similar results were later obtained by Kveder et al. [5] in the case of both n- and p-type silicon, also subjected to the plastic deformation. They noticed several overlapping DLTS lines in preliminarily deformed, but not annealed samples, which were much broader than those typically observed for point defects. They concluded that the traps may be associated to the dislocation core or point defects surrounding the dislocation. After annealing, only one distinctly broadened line remains in the DLTS spectra, and its amplitude shows an anomalous logarithmic dependence on the duration of the refilling pulses (see Sec. 5) [5]. The authors explained these observed changes by the reconstruction of most of the dangling bonds in the dislocation core. Anomalous symmetrical line broadening was also studied by Omeling et al. [6] for a deep electron trap in  $\text{GaAs}_{1-x}\text{P}_x$  ternary compound alloys, labelled as the well known EL2-level. This effect was attributed to the dispersion of energy level positions of the defect in the band gap, as a result of varying alloy composition in the crystal. In the proposed model of broadened deep levels, the Gaussian distribution function was used, with the standard deviation of the distribution considered as the broadening parameter. In this model, it was shown that the thermal emission rates and mean values of activation energies can be obtained in a similar way as in conventional DLTS analysis, although the transients are strongly non-exponential. This causes the distortion of DLTS peaks. Moreover, the energy

distribution and corrected deep trap concentration can be calculated from the DLTS spectra observed experimentally [6]. This approach was also predicted to be useful, even when the defect levels are broadened for reasons different than varying alloy composition, such as inhomogeneous strain field distribution in crystals or defect interaction.

This model has also been successfully applied to analysing dislocation-related DLTS peaks in plastically deformed silicon for which symmetrical line broadening was also observed [7]. The DLTS spectra observed in PD silicon were ascribed by Kisielowski et al. [19] to the deformation-induced disorder on the energy level and capture cross section of point defect clouds surrounding dislocations. A few years later, these results were confirmed by Cavalcoli et al. [20] for the same traps observed in PD silicon. The authors paid particular attention to the broadened DLTS peak, labelled C. With regard to its peculiar features, such as shape dependence on the deformation procedure, an increase of concentration with dislocation density, and domination at high deformation temperature, etc., they concluded this trap to be most probably localized at dislocations, while other traps to be mainly due to deformation-induced point defects surrounding dislocations or left behind dislocations during their motion [20].

In n-type GaAs exposed to plastic deformation, Wosiński [8] has also detected a broadened asymmetric DLTS peak, evoked by an electron trap labelled ED1. It is worth noticing that, unlike previously observed deep traps in plastically deformed Si [7], generally attributed to point defect clouds around the dislocation line, the trap in GaAs was considered to be closely related to the core states of  $60^\circ$ -dislocations [8].

The broadened DLTS peaks associated with dislocations are typically observed in SiGe heterostructures [21–23] and ternary compound systems like InGaAs [24–26] and GaAsSb [27, 28]. They are caused by a lattice mismatch between the substrate and epitaxial layer. This leads to the formation of misfit dislocations at the interface, accompanied by threading dislocations [29,30]. Broad DLTS peaks were also recently observed in quaternary compound heterostructures like InGaAsN [31], and were associated either with continuous distributions of states, typical of extended defects, or with groups of closely spaced discrete energy levels.

Unfortunately, there is a wide set of other phenomena that cause significant distortions in conventional DLTS spectra and thereby add complexity to the DLTS formalism. Non-exponential capacitance transients are known to arise in the case of (i) high trap concentrations compared to shallow level doping [32], (ii) closely spaced, multiple deep levels with comparable emission rates [33], (iii) strong electric fields that influence trap emission [34], (iv) capture from free-carrier tails in a depletion region [18], and (v) inhomogeneous carrier concentrations [35]. A superposition of some peaks related to specific clusters of point defects is also one of the observed reasons for the broadening and anomalous behaviour of so-called U-shaped peaks [36]. Therefore, deep level transient spectroscopy requires a careful analysis when broadened spectra are observed.

A common problem appearing when deep impurity levels are studied in compound semiconductors by means of DLTS is the so-called alloy broadening. Semiconductor alloys such as  $\text{GaAs}_x\text{Sb}_{1-x}$ ,  $\text{GaAs}_x\text{P}_{1-x}$ , and  $\text{Al}_x\text{Ga}_{1-x}\text{As}$ , and other disordered structures, are substitutionally disordered systems in which the main reason for disorder is the presence of composition fluctuations due to a random distribution of group V atoms in the corresponding sublattice. In such cases, the DLTS spectrum may be broadened and the corresponding capacitance transients may be non-exponential, because of deep level energy spectrum broadening [37]. Broadened DLTS spectra connected with alloy composition fluctuations have already been studied in GaAsP [6, 38], GaAsSb [39, 40], and other disordered systems such as moderately doped GaAs [41].

#### 4. DLTS line amplitude behaviour analysis – “localized” and “bandlike” states

Spatially extended defects, owing to their many-electron character, are associated with a large number of electronic states in the band gap. They form deep-lying one-dimensional energy bands rather than isolated energy levels, typically attributed to point defects. The nature of DLTS lines in the case of extended defects can be investigated within the model developed by Schröter et al. [10–13]. This model (Fig. 1) has revealed that extended defects may be associated with [12]: (i) a density of states  $N_d(E)$  that leads to DLTS line broadening, (ii) a capture barrier  $\delta E_C$ , which changes with the defect charge and modifies the capture rate, (iii) an internal equilibration time  $\Gamma_i$  (i.e., the time needed to attain an internal electronic equilibrium of the defect), which affects the filling pulse dependence of the line shape.

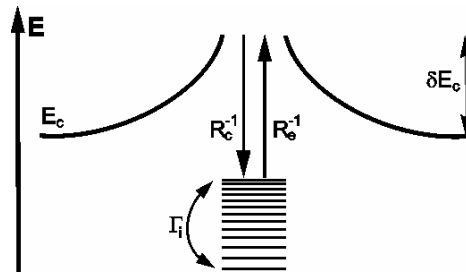


Fig. 1. Band diagram of electronic states at an extended defect [12].

The capture barrier  $\delta E_C$ , the internal equilibration time  $\Gamma_i$ , inverse rates of carrier emission and capture,  $R_e^{-1}$  and  $R_c^{-1}$ , respectively, are shown in the figure

Considering the internal equilibration time  $\Gamma_i$ , some authors [10–13] have demonstrated that deep-lying electronic states at extended defects can be classified as “localized” or “band-like”. By comparing the time  $\Gamma_i$  with the inverse carrier emission rate  $R_e^{-1}$  and the inverse of the carrier capture rate defects  $R_c^{-1}$  (the time needed to reach

equilibrium with conduction and valence bands), the distinction between “localized” and “bandlike” density of states can be made. When  $\Gamma_i \gg R_e^{-1}, R_c^{-1}$ , i.e. the internal electron exchange rate is small, the states are named “localized”, whereas in the case of a large internal electron exchange rate, namely when  $\Gamma_i \ll R_e^{-1}, R_c^{-1}$ , states are “bandlike”.

In the area of DLTS measurements, the criteria designed for distinguishing between these two types of states have been established [10, 11]. They concern the variation of the DLTS line maximum and its shape with the filling-pulse duration  $t_p$ . For “localized” states, while changing the filling-pulse duration: (i) the maximum of the DLTS line amplitude stays almost constant, (ii) the high-temperature side of DLTS lines generally coincide after normalizing, (iii) the DLTS line amplitude exhibits a linear dependence on the logarithm of the filling time (Sec. 5). On the contrary, in the case of “bandlike” states, the variation of the filling-pulse time length leads to the following: (i) the maximum of the DLTS line amplitude shifts to lower temperatures on increasing the duration, (ii) the high-temperature side of DLTS – lines coincide, (iii) the DLTS line amplitude exhibits a linear dependence on the logarithm of the filling time (Sec. 5). It is important that in both cases the DLTS line amplitudes are broadened, a typical feature in the case of extended defects (Sec. 3).

Applying the above criteria, “localized” deep electronic states have already been revealed in the case of 60° dislocations in plastically deformed silicon [10], whereas electronic states at dislocation rings bounding nanoscale NiSi<sub>2</sub> precipitates in silicon [12] have been related to the “band-like” class of states. A behaviour similar to the “localized” case was experimentally observed by Panepinto and Yastrubchak for the same electron trap in lattice-mismatched InGaAs/GaAs heterostructures grown by MOVPE [24] and MBE [42]. These traps were attributed to narrow clouds of point defects around dislocations and threading dislocations in the layer, respectively. “Bandlike” states have also been observed in the same heterostructures, for a deep hole trap associated with misfit dislocations at the InGaAs/GaAs interface [42].

A conventional analysis of the DLTS spectra for extended defects allows us to determine the apparent values of activation energy and capture cross section, but the interpretation of the obtained parameters is not as obvious as for isolated point defects. While point traps may produce distinct peaks for every trap, a distribution of energetically close traps may produce a single broadened peak [2, 7, 21]. Its thermal emission rate is a weighted average value of the emission rates of all the traps contributing to the peak at a given temperature. According to Grillot et al. [22], the lowest energy states make a dominant contribution to the high-temperature edge of the DLTS peak, whereas the highest-energy states make a dominant contribution to the low-temperature edge of the DLTS peak. Furthermore, for short filling-pulse times, the lowest-energy states are filled first, causing a broadening of the DLTS peak on its low-temperature side with increasing filling-pulse duration. Furthermore, the Arrhenius plots for extended defects differ significantly for different filling-pulse times. Hedemann et al. [11] have shown that apparent activation energies and capture cross sections obtained from Arrhenius plot analyses cannot be treated as average values for



the distribution of levels. The determined parameters should be reported together with the measurement parameters, especially with the filling-pulse length.

It should be noticed that the behaviour of the DLTS signal in the case of isolated point defects can also be taken into account, but less forcibly, mainly as a factor discriminating them from spatially extended effects. Namely, the DLTS signal originating from deep levels and associated with point traps does not show any changes in its peak positions on increasing the filling-pulse duration, while the observed DLTS peak shape is typically narrow and symmetric.

## 5. Capture kinetics analysis

The main specific feature of DLTS lines, usually considered to be the fingerprint of extended defects, particularly dislocations, is the so-called logarithmic capture law, i.e., a logarithmic dependence of the kinetics for majority charge carriers captured in trap states. Such a law was observed experimentally for the first time by Figielski in plastically deformed Ge and Si [43]. In this paper, it is shown that the steady-state photoconductivity increases linearly with the logarithm of the light intensity over a wide range of illumination. It was also noticed that photoconductivity decayed logarithmically in time after illumination by a rectangular light pulse. The observed phenomena were explained in terms of a barrier model of recombination processes via dislocations. In this model, the capture rate of free charge carriers, limited by a Coulombic barrier of the repulsive electrostatic potential built up at the defect, is proportional to the number of electrons already captured at the dislocation line [8, 43]. Such a dependence can occur when the trap levels are arranged in a linear array, interacting between themselves, and not randomly distributed in the whole crystal.

Furthermore, it turned out that the mentioned phenomena can be successfully observed by the DLTS technique [8]. Today this is exploited in DLTS measurements as a principal argument for discriminating between isolated points and extended traps, which can be expressed as a linear dependence of the DLTS peak amplitude on the logarithm of the filling-pulse duration [8]. This effect has already been observed for dislocations in plastically deformed Si [7, 9, 20] and GaAs [8]. It is also observed in the case of lattice-mismatched heterostructures, like SiGe [21–23], InGaAs [24–26, 42, 44], and GaAsSb [27, 28].

On the contrary, isolated point defects or impurities typically reveal exponential capture kinetics (the exponential capture law). This dependence can also be investigated by DLTS. In this case, a characteristic distinct saturation of the DLTS peak amplitude for long filling-pulse durations is observed [45]. Such a behaviour is typical of noninteracting point defects. As the DLTS amplitude is proportional to the defect concentration, the time at which saturation is reached describes the situation when no more free charge carriers are captured in defect states. Therefore, it determines the trap concentration  $N_T$ .

In capture kinetics measurements it is difficult to avoid experimental problems leading to incorrect results. The free-carrier tail effect during the capture process, the

so-called capture in the Debye tail, is a commonly appearing problem. This effect causes the non-exponential character of the capacitance transients. A detailed analysis of capture kinetics measurements was carried out by Pons [18], according to whom capture in the Debye tail contributes slightly to the fast exponential kinetics, changing with the logarithm of the filling-pulse duration. As a result of this contribution, no distinct saturation of the DLTS amplitude with increasing filling time is observed. In order to extract the exponential capture kinetics from the total kinetics, namely getting rid of the capture in the Debye tail and obtaining a correct estimation of the capture rate, a novel fitting model has been proposed [18]. This model was successfully used in measurements of thermally activated capture cross sections [45].

Furthermore, non-exponential thermal emission and capture kinetics are also generally observed in the case of donor-related defects – so-called DX centres – present in many III–V compound semiconductors. Systematic studies of such anomalous emission and capture transients on DX centres have shown that they may be due to various effects, such as a random distribution of atoms in the crystal lattice (alloy broadening) [46, 47], concentrations of DX centres equal to shallow impurity doping [48], or large lattice relaxation [14]. Therefore, a possible existence of DX centres in the investigated heterostructure has also be taken into account when analysing DLTS signals.

It should also be noticed that low-dimensional systems in semiconductor heterostructures, such as quantum wells (QW) and quantum dots (QD), can also evoke some non-classical effects in the emission and capture of charge carriers. These are typically expected to be viewed as spatially extended defects and thereby characterized by the DLTS technique. It is generally known that in DLTS measurements a single quantum well (SQW) acts electrically as a deep level trap, a so-called “giant trap”, because it can capture and emit free carriers from well regions in the same way as a deep trap [49, 50]. Quantum dots (QDs), as quasi-zero-dimensional structures, should behave even more like a classical point defect than quantum wells. The quantisation of energy levels, however, should be taken into account in such low dimensional systems. Thus, the presence of QWs and QDs in compound semiconductors may produce effects that significantly affect the DLTS formalism. Similarly to extended defects, they show symmetrically or asymmetrically broadened DLTS peaks or the non-exponential capture and emission characteristics of free carriers [49–52].

## 6. Summary – setting up the criteria

We have already presented some crucial results and remarks brought up in a large number of papers. They involved investigations and analyses of peculiar features in DLTS signals originating from deep level traps, associated with both point and extended defects in semiconductor materials. We would like to gather all the mentioned information in order to outline a compact scheme of criteria, making it possible, in

a simple way, to distinguish between isolated point defects and extended defects in DLTS measurements.

In the case of point defects, one can usually observe:

- narrow and symmetric peaks (Sec. 3),
- stability of the DLTS peak maximum with increasing filling pulse duration (Sec. 4),
- exponential capture kinetics (the exponential capture law) (Sec. 5).

For extended defects, a DLTS signal reveals completely opposite features:

- symmetrically or asymmetrically broadened peaks (Sec. 3),
- dependence of the DLTS peak maximum on increasing duration and on the type of electronic state at the extended defect (Sec. 4):
  - for “localized” states, the DLTS line maximum stays almost constant and its high-temperature side coincides after normalizing,
  - for “bandlike” states, the DLTS line maximum shifts to lower temperatures and, simultaneously, its high-temperature side coincides,
  - logarithmic capture kinetics (the logarithmic capture law) (Sec. 5).

In our opinion, the presented facts can be successfully exploited for studying all types of extended defects, including all kinds of dislocations as the most commonly encountered representatives of that “species” of defects. Therefore, the conventional analysis of DLTS data, which makes it possible to obtain all deep level parameters (i.e., thermal emission rates, activation energies, capture cross sections, and concentrations) and to describe their dependencies on the electric field or temperature, can be extended by a more detailed analysis of the nature of the deep level defects observed in semiconductors. The comparison of DLTS data analysis and conclusions drawn from previous reports of dislocation-related deep level states is also indispensable. It is crucial, however, to exclude other numerous phenomena that can affect the DLTS signal coming from samples and cause serious misinterpretations in the analyses of spectra.

## 7. Experimental identification of extended defects in $A^{III}B^V$ semiconductors

DLTS investigations of two kinds of samples, lattice-matched n-GaAs/GaAs (sample A) and lattice-mismatched n-In<sub>0.085</sub>Ga<sub>0.915</sub>As/GaAs (sample B), were performed. The samples were grown by the MOVPE method. In order to make the DLTS measurements possible, Schottky contacts were prepared by a standard lift-off technique on top of the samples, and ohmic contacts on their back sides. All the technological details concerning sample preparation are given elsewhere [53, 54]. The quality of the Schottky barriers was checked by  $I$ – $V$  and  $C$ – $V$  measurements, which indicated good rectifying characteristics. The DLTS measurements were performed

by means of a lock-in type spectrometer DLS-82E, manufactured by Semitrap, Hungary [55]. Conventional DLTS [2] as well as double correlation DLTS methods [16] were applied in our investigations.

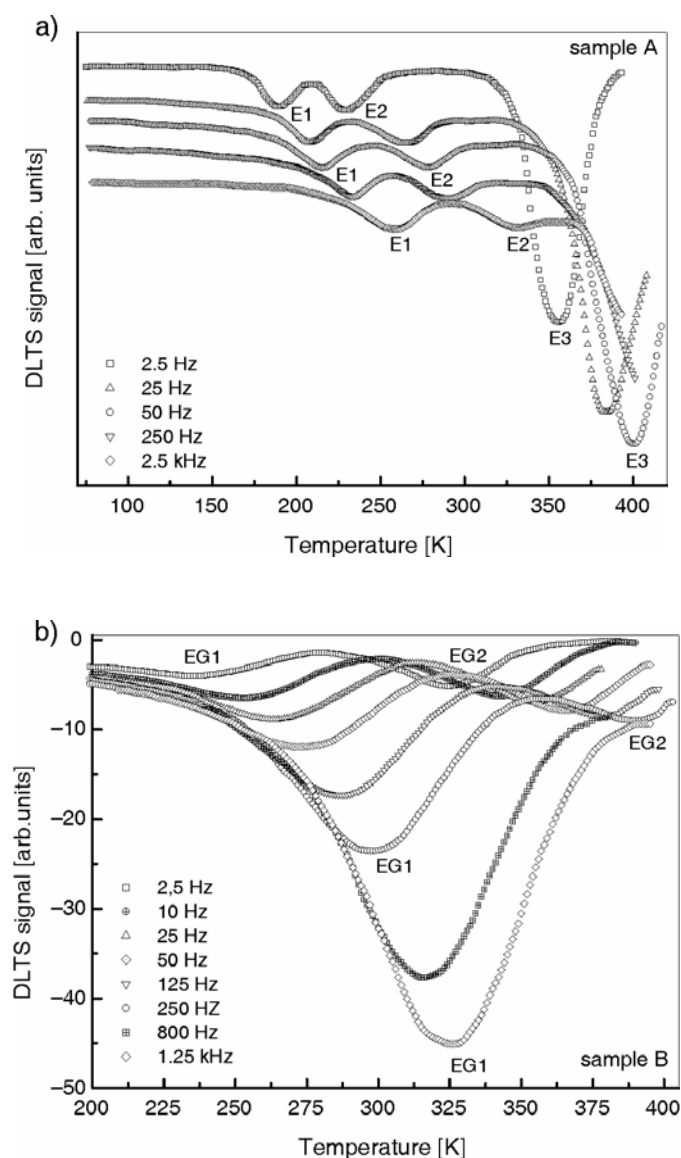


Fig. 2. DLTS temperature spectra of: a) a GaAs/GaAs structure for several lock-in frequencies measured in the conventional DLTS mode in the 77–410 K temperature range; reverse bias was  $U_R = -3$  V, filling pulse height  $U_1 = -0.5$  V, and the width of the pulse 20  $\mu$ s; scans were vertically moved between themselves for clarity, b) a  $\text{In}_{0.085}\text{Ga}_{0.915}\text{As}/\text{GaAs}$  system for several lock-in frequencies, measured in the DDLTS mode in the 200–400 K temperature range; reverse bias was  $U_R = -1$  V, filling pulse heights  $U_1 = 0$  V and  $U_2 = -0.5$  V, and the widths of the pulses 20  $\mu$ s

Example DLTS temperature spectra of the two samples, for several different lock-in frequencies, are given in Fig. 2. Three deep electron traps, labelled E1, E2, and E3, are present in the GaAs/GaAs sample (Fig. 2a), and two electron traps, labelled EG1, EG2, in  $\text{In}_{0.085}\text{Ga}_{0.915}\text{As}/\text{GaAs}$  sample (Fig. 2b). The latter sample was grown in lattice mismatch conditions between the epitaxial layer and substrate. The calculated lattice misfit parameter amounted to about 0.6%, resulting in the generation of a network of two-dimensional  $60^\circ$  misfit dislocations, typically lying along two orthogonal  $\langle 110 \rangle$  directions at the (001) interface [44]. The DLTS lines of the EG1 trap (Fig. 2b) are distinctly broadened, as opposed to all the other traps presented in both samples. In accordance with the previous information, non-exponential transients connected with the electronic states of dislocations can bring about such as broadening. For sample A, all the DLTS peaks are narrow and symmetric, because only isolated point defects, and no dislocations, were expected to appear in such a structure.

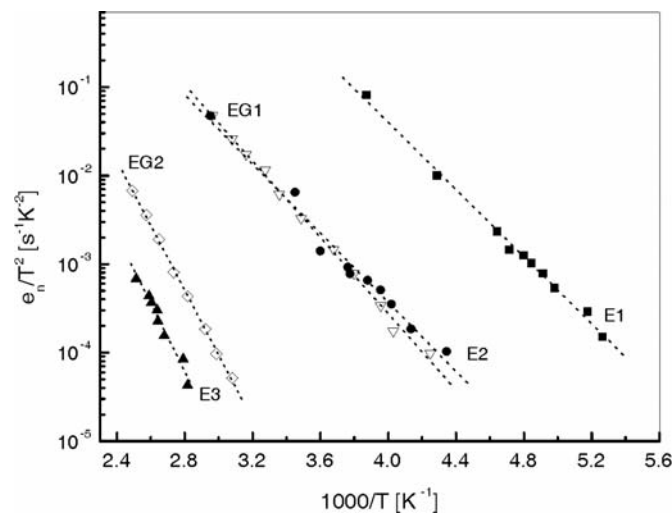


Fig. 3. Temperature dependence of the thermal emission rates (Arrhenius plots) for all the electron traps revealed in GaAs/GaAs (solid symbols) and  $\text{In}_{0.085}\text{Ga}_{0.915}\text{As}/\text{GaAs}$  (open symbols). The dotted lines show the best least-squares fit to the experimental data

Taking the temperature scans from Fig. 2, Arrhenius plots can be constructed, i.e. temperature dependences of the emission rates for each trap in both samples (Fig. 3). The activation energies  $E_a$  and capture cross sections  $\sigma_n$ , obtained by means of the standard least-squares fitting procedure, are given in Table 1.

The DLTS line of the trap EG1 is broadened and no saturation is observed up to the longest filling-pulse time used in the experiment (Fig. 4). Such behaviour (the logarithmic capture law), as mentioned in previous sections, is the most characteristic feature of extended defects due to carrier capture being limited by an occupation-dependent barrier [43]. Indeed, after carrying out capture kinetics measurements it turned out that the amplitude of the dominant EG1 line in sample B exhibits a linear

dependence on the logarithm of the filling time, as presented in Fig. 5. Furthermore, no distinct shift of the EG1 peak was observed and a normalized plot of the peak revealed that its high temperature sides match to each other (Fig. 4). This enables us to attribute the EG1 trap to “localized” states at the dislocation core or very close to it.

Table 1. Activation energies  $E_a$  and capture cross sections  $\sigma_n$  for traps revealed in samples A and B, determined from Arrhenius plots (Fig. 3) using a filling pulse duration of  $t_p = 20 \mu\text{s}$

Sample	Trap	$E_a$ [eV]	$\sigma_n$ [ $\text{cm}^2$ ]	Identification
A	E1	0.38	$9.1 \times 10^{-15}$	point defect (EL5)
	E2	0.41	$2.6 \times 10^{-16}$	point defect (EI1)
	E3	0.76	$1.5 \times 10^{-14}$	native point defect (EL2)
B	EG1	0.43	$5.73 \times 10^{-16} *$	misfit dislocation (ED1)
	EG2	0.72	$4.22 \times 10^{-14}$	native point defect (EL2)

\*The value changes with time.

The dislocation trap, labelled EG4, associated with localized states at dislocations, was previously observed in MOVPE grown GaAs/InGaAs/GaAs single-quantum wells by Panepinto et al. [24], who ascribed this trap to misfit dislocations close to the interface in the GaAs buffer layer. The trap was identified by the authors as ED1, and was found for the first time in plastically deformed GaAs by Wosiński [8], then in GaAsSb/GaAs [27], and recently in InGaAs/GaAs [26, 42] lattice-mismatched heterostructures. The activation energy of the trap ED1, equal to 0.68 eV, is much higher than our results for the trap EG1 shown in Table 1 (0.43 eV). We believe our trap has a similar origin as ED1. The difference in activation energies may result from the fact that, as mentioned in Section 4, the measured activation energies (Arrhenius plot) differ significantly for various fixed filling-pulse durations. In this paper, all the activation energies were measured with a filling-pulse time of  $t_p = 20 \mu\text{s}$ , but the value of  $t_p$  used by Wosiński is not known. Furthermore, there are other reasons, such as different growth techniques or indium content, etc. In order to clearly identify the origin of the EG1 trap, further investigations are needed.

On the contrary, it can be seen in Figs. 4 and 5 that the DLTS line of the second electron trap EG2 in sample B shows a distinct saturation for long filling times, characteristic of non-interacting isolated point defects (the exponential capture law). Identical behaviour was also observed for sample A in the case of the dominant trap labelled E3. Moreover, these two traps, E3 and EG2, were identified on the basis of their parameters obtained from Arrhenius plots (Fig. 3). These parameters (Table 1) are very similar to those of the trap EL2 [56] – the dominant native defect in GaAs, identified as an As-antisite defect ( $\text{As}_{\text{Ga}}$ ). For the traps E1 and E2, capture kinetics measurements have not been performed, because they revealed saturation already for very short filling-pulse times. From the emission characteristics of the two traps, it

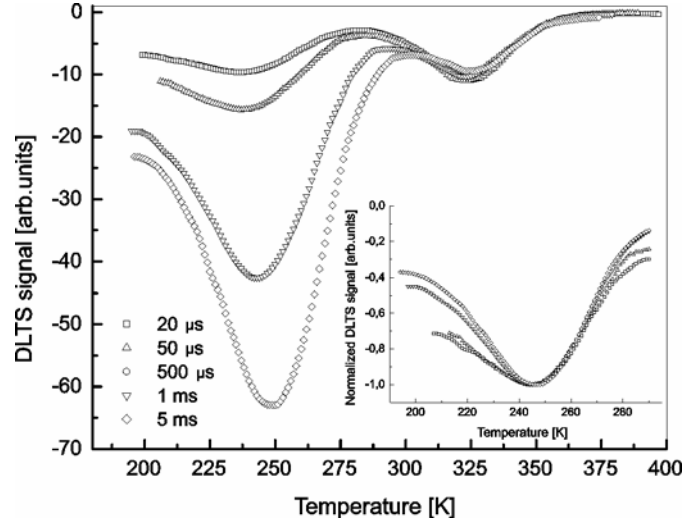


Fig. 4. DLTS temperature spectra of the  $\text{In}_{0.085}\text{Ga}_{0.915}\text{As}/\text{GaAs}$  heterostructure for different filling pulse times. Reverse bias was  $U_R = -1$  V, filling pulses heights  $U_1 = 0$  V and  $U_2 = -0.5$  V, and the lock-in frequency constant at 2.5 Hz. The inset shows the plot of the normalized DLTS peak amplitude of the trap EG1

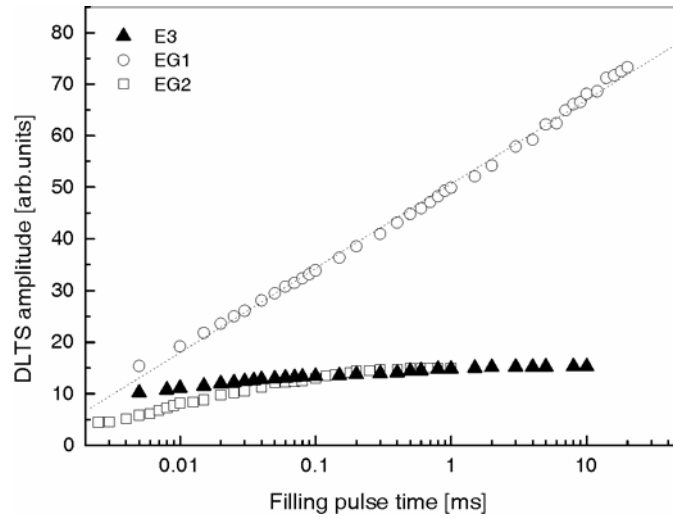


Fig. 5. DLTS peaks amplitudes of the trap E3 (solid symbols) in GaAs/GaAs, and EG1 and EG2 (open symbols) in  $\text{In}_{0.085}\text{Ga}_{0.915}\text{As}/\text{GaAs}$  as functions of the filling-pulse time

was possible to identify them as the traps EL5 [56] and EI1 [16], respectively. All the deep level parameters determined for each trap in both samples are summarized in Table 1. It is worth noticing that the carrier capture cross section evaluated for the dislocation trap EG1 (Table 1) changes with time. This results from the fact that, by

definition, the capture cross section of an extended defect changes with time – as the charge builds up, the defect becomes less attractive.

## 8. Conclusions

In conclusion, criteria concerning distinguishing between point and extended defects, especially dislocations, in DLTS experiments have been presented. Criteria containing DLTS line shape and behaviour analysis, as well as capture kinetics measurements, allow us to clearly differentiate between these two types of defects. These exceptional features of point and extended defects encountered in DLTS measurements have been exploited in the analysis and identification of deep level defects in lattice-matched n-GaAs/GaAs and lattice-mismatched n-In<sub>0.085</sub>Ga<sub>0.915</sub>As/GaAs heterostructures. All deep levels have been identified on the basis of their parameters and the odd features of their DLTS line spectra. The possible association of the trap EG1, revealed in this work in lattice-mismatched samples, with the dislocation trap labelled ED1 in literature, is not obvious and requires further investigations.

## References

- [1] WEBER E.R., *Physica B*, 340–342 (2003), 1.
- [2] LANG D.V., *J. Appl. Phys.*, 45 (1974), 3023.
- [3] FIGIELSKI T., *Phys. Stat. Sol. (a)*, 121 (1990), 187.
- [4] KIMERLING L.C., PATEL J.R., *Appl. Phys. Lett.*, 34 (1979), 73.
- [5] KVEDER V.V., OSIPYAN YU.A., SCHÖTER W., ZOTH G., *Phys. Stat. Sol. (a)*, 72 (1982), 701.
- [6] OMLING P., SAMUELSON L., GRIMMEISS H.G., *J. Appl. Phys.*, 54 (1983), 5117.
- [7] OMLING P., WEBER E.R., MONTELIUS L., ALEXANDER H., MICHEL J., *Phys. Rev. B*, 32 (1985), 6571.
- [8] WOSIŃSKI T., *J. Appl. Phys.*, 65 (1989), 1566.
- [9] SCHRÖTER W., QUEISSER I., KRONWITZ J., *Inst. Phys. Conf. Ser.*, 104 (1989), 75.
- [10] SCHRÖTER W., KRONWITZ J., GNAUERT U., RIEDEL F., SEIBT M., *Phys. Rev. B*, 52 (1995), 13726.
- [11] HEDEMAN H., SCHRÖTER W., *J. Phys. III France*, 7 (1997), 1389.
- [12] RIEDEL F., SCHRÖTER W., *Phys. Rev. B*, 62 (2000), 7150.
- [13] SCHRÖTER W., HEDEMAN H., KVEDER V., RIEDEL F., *J. Phys. Condens. Matter.*, 14 (2002), 13047.
- [14] SCHUBERT E.F., *Doping in III–V Semiconductors*, Cambridge Univ. Press, 1993.
- [15] SCHRODER D.K., *Semiconductor Material and Device Characterization*, Wiley, New York, 1990.
- [16] LEFEVRE H., SCHULZ M., *Appl. Phys.*, 12 (1977), 45.
- [17] HENRY C.H., LANG D.V., *Phys. Rev. B*, 15 (1977), 989.
- [18] PONS D., *J. Appl. Phys.*, 55 (1984), 3644.
- [19] KISIELOWSKI C., WEBER E.R., *Phys. Rev. B*, 44 (1991), 1600.
- [20] CAVALCOLI D., CAVALLINI A., GOMBIA E., *J. Phys. III France*, 7 (1997), 1399.
- [21] GRILLOT P.N., RINGEL S.A., FITZGERALD E.A., WATSON G.P., XIE Y.H., *J. Appl. Phys.*, 77 (1995), 676.
- [22] GRILLOT P.N., RINGEL S.A., FITZGERALD E.A., WATSON G.P., XIE Y.H., *J. Appl. Phys.*, 77 (1995), 3248.
- [23] CHRETIEN O., APETZ R., VESCAN L., *Semicond. Sci. Technol.*, 11 (1996), 1838.
- [24] PANEPINTO L., ZEIMER U., SEIFERT W., SEIBT M., BUGGE F., WEYERS M., SCHRÖTER W., *Mater. Sci. Eng. B*, 42 (1996), 77.
- [25] PAL D., GOMBIA E., MOSCA R., BOSACCHI A., FRANCHI S., *J. Appl. Phys.*, 84 (1998), 2965.



- [26] WOSIŃSKI T., YASTRUBCHAK O., MAKOSA A., FIGIELSKI T., *J. Phys.: Condens. Matter*, 12 (2000), 10153.
- [27] WOSIŃSKI T., MAKOSA A., FIGIELSKI T., RACZYŃSKA J., *Appl. Phys. Lett.*, 67 (1995), 1131.
- [28] PŁACZEK-POPKO E., SZATKOWSKI J., HAJDUSIAŃEK A., RADOJEWSKA B., *Proc. SPIE*, 2780 (1996), 153.
- [29] TE NIJENHUIS J., VAN DER WEL P.J., VAN ECK E.R.H., GILING L.J., *J. Phys. D: Appl. Phys.*, 29 (1996), 2961.
- [30] LIU X.W., HOPGOOD A.A., USHER B.F., WANG H., BRAITHWAITE N.St.J., *Semicond. Sci. Technol.*, 14 (1999), 1154.
- [31] KAPLAR R.J., RINGEL S.A., KURTZ S.R., KLEM J.F., ALLERMAN A.A., *Appl. Phys. Lett.*, 80 (2002), 4777.
- [32] STIEVENARD D., LANNOO M., BOURGOIN J.C., *Solid-State Electron.*, 28 (1985), 485.
- [33] IKOSI-ANASTASIOU K., ROENKER K.P., *J. Appl. Phys.*, 61 (1987), 182.
- [34] SAH C.T., *Solid-State Electron.*, 19 (1976), 975.
- [35] ITO A., TOKUDA Y., *Solid-State Electron.*, 46 (2002), 1307.
- [36] BRUDNYI V.N., PESHEV V.V., *Semiconductors*, 37 (2003), 140.
- [37] DAS A., SINGH V.A., LANG D.V., *Semicond. Sci. Technol.*, 3 (1988), 1177.
- [38] KANIEWSKA M., KANIEWSKI J., *Solid State Commun.*, 53 (1985), 485.
- [39] DIWAN A., SINGH V.A., ARORA B.M., MURAWALA P.A., *J. Phys C: Solid State Phys.*, 20 (1987), 3603.
- [40] WOSIŃSKI T., MAKOSA A., RACZYŃSKA J., *Acta Phys. Polon. A*, 79 (1995), 369.
- [41] HARDALOV CH., YANCHEV I., GERMANOVA K., IVANOV TZV., SAMURKOVA L., KIRKOV K., NIGOHOSEAN A., *J. Appl. Phys.*, 71 (1992), 2270.
- [42] YASTRUBCHAK O., WOSIŃSKI T., MAKOSA A., FIGIELSKI T., TÓTH A.L., *Physica B*, 308-310 (2001), 757.
- [43] FIGIELSKI T., *Solid State Electron.*, 21 (1978), 1403.
- [44] WATSON G.P., AST D.G., ANDERSON T.J., PATHANGAY B., HAYAKAWA Y., *J. Appl. Phys.*, 71 (1992), 3399.
- [45] SZATKOWSKI J., PŁACZEK-POPKO E., SIERAŃSKI K., HANSEN O.P., *J. Appl. Phys.*, 86 (1999), 1433.
- [46] CALLEJA E., MOONEY P.M., WRIGHT S.L., HEIBLUM M., *Appl. Phys. Lett.*, 49 (1986), 657.
- [47] MOONEY P.M., CASWELL N.S., WRIGHT S.L., *J. Appl. Phys.*, 62 (1987), 4786.
- [48] BOURGOIN J.C., FENG S.L., BARDELEBEN H.J., *Appl. Phys. Lett.*, 53 (1988), 1841.
- [49] WANG A.Z., ERSEREN W.A., *Solid-State Electronics*, 38 (1995), 673.
- [50] YOON S.F., LUI P.Y., ZHENG H.Q., *J. Cryst. Growth*, 212 (2000), 49.
- [51] WALTHER C., BOLLMANN J., KISIEL H., KRIMSE H., NEUMANN W., MASSELINK W.T., *Physica B*, 273-274 (1999), 971.
- [52] GOMBIA E., MOSCA R., FRIGERI P., FRANCHI S., AMIGHETTI S., GHEZZI C., *Mat. Sci. Eng. B*, 91 (2002), 393.
- [53] GELCZUK Ł., DĄBROWSKA-SZATA M., *Elektronika*, 10 (2003), 3.
- [54] GELCZUK Ł., DĄBROWSKA-SZATA M., JÓŹWIĄK G., RADZIEWICZ D., *Acta Phys. Polon. A*, 106 (2003), 265.
- [55] FERENCZI G., KISS J., *Acta Phys. Acad. Sci. Hung.*, 50 (1981), 285.
- [56] MARTIN G.M., MITONNEAU A., MIRCEA A., *Electron. Lett.*, 13 (1977), 191.

*Received 10 May 2005*

*Revised 27 July 2005*